

## **Photoinduced dichroism and birefringence in films of Mordant Pure Yellow/poly(vinyl alcohol): simultaneous real-time investigations at two wavelengths**

M. IVANOV, L. NIKOLOVA, T. TODOROV, N. TOMOVA,  
V. DRAGOSTINOVA

*Central Laboratory of Optical Storage and Processing of Information,  
Bulgarian Academy of Sciences, P.O. Box 95, Sofia 1113, Bulgaria*

*Received 7 November 1993; revised 16 March; accepted 24 March 1994*

---

Photoinduced anisotropy in films of azo-dye Mordant Pure Yellow (MPY) dissolved in a polyvinyl alcohol matrix, is investigated. The photodichroism and photoinduced birefringence are measured in real time for two wavelengths, 488 nm (in the absorption band) and 633 nm (outside it), on excitation with an Ar<sup>+</sup> laser beam. It is shown that strong dichroism is induced without changing the average optical density of the film, and the kinetic curves of the birefringence and the dichroism are substantially different. The conclusion is made that the photoprocesses of the dye molecules cause a reconstruction of the matrix.

---

### **1. Introduction**

In recent years, photoinduced optical anisotropy in polymer/organic dye systems has been the object of intensive investigations. These materials are promising for the purposes of modern optics: for optical recording, optically-controlled optical elements, optical switches, and so on. In the most prominent of these systems, the dye is of the azo-aromatic type and the anisotropy is caused by photoinduced *trans*–*cis* isomerization and ordering of the absorbing molecules' axes in directions in which light affects them less [1–10]. The azo-dye may be simply dissolved in the polymer [1–5] or linked by a covalent bond to the polymer chain [6–10]. It may have one or more nitrogen double bonds and the aromatic groups may be benzene or other nuclei. This diversity affects the characteristics of the photoprocesses.

Particularly large values of induced birefringence are observed in films of the dye Mordant Pure Yellow (MPY) dissolved in a matrix of poly(vinyl alcohol) (PVA) or gelatin [2–5]. The molecular structure of this azo-dye is shown in Fig. 1.

Birefringent gratings recorded in MPY/PVA samples have diffraction efficiency close to 100% [2]. The investigations [2–4] involved spectra and exposure characteristics of anisotropy in these materials. The exact mechanism of inducing the birefringence in such films is unclear. It is unknown whether it is related solely to ordering of the dye molecules and the corresponding dichroism in the absorption band, or to simultaneous restructuring of the polymer matrix.

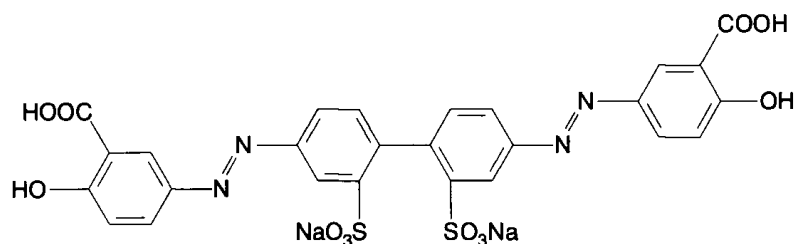


Figure 1 Structure of Mordant Pure Yellow.

In the present work we report results from simultaneous kinetic investigations on photo-induced dichroism and birefringence in samples of MPY/PVA, measured simultaneously at two wavelengths, within and outside the absorption band.

## 2. Experimental

Films using rigid solutions of MPY dye in different concentrations in a PVA matrix were prepared. Several types of PVA (Readel, Fluka) with different molecular weights were utilized. The dye was dissolved in a water solution of PVA and the films were deposited on glass substrates. The samples were dried for 24 h at 20°C. The investigations were carried out with samples of Fluka of molecular weight 100 000 and dye concentration 5 wt%. The sample thickness was 50  $\mu\text{m}$  and the absorption maximum was at 380 nm. The experimental setup allowed simultaneous measurement of the kinetics of the photoinduced birefringence and dichroism at  $\lambda = 633 \text{ nm}$  and dichroism at  $\lambda = 488 \text{ nm}$  (Fig. 2). In the experiment, the sample S is illuminated by the linearly (vertically) or circularly polarized beam 1 from an  $\text{Ar}^+$  laser of  $\lambda = 488 \text{ nm}$ . Its polarization is varied with a Babinet–Soleil compensator B. Beam 2 from the  $\text{Ar}^+$  laser is directed to the sample S via beam splitter BS2 and shutter C. Beam 3 from the He–Ne laser is directed to the sample S via beam splitter BS3 and polarizer P3. The sample S is analyzed by a photopolarimeter PP and a Wollaston prism W, which directs the light to detectors R6 and R7. Detectors R5, R6, R7, and R8 are positioned at various points in the setup to measure the intensity of the beams.

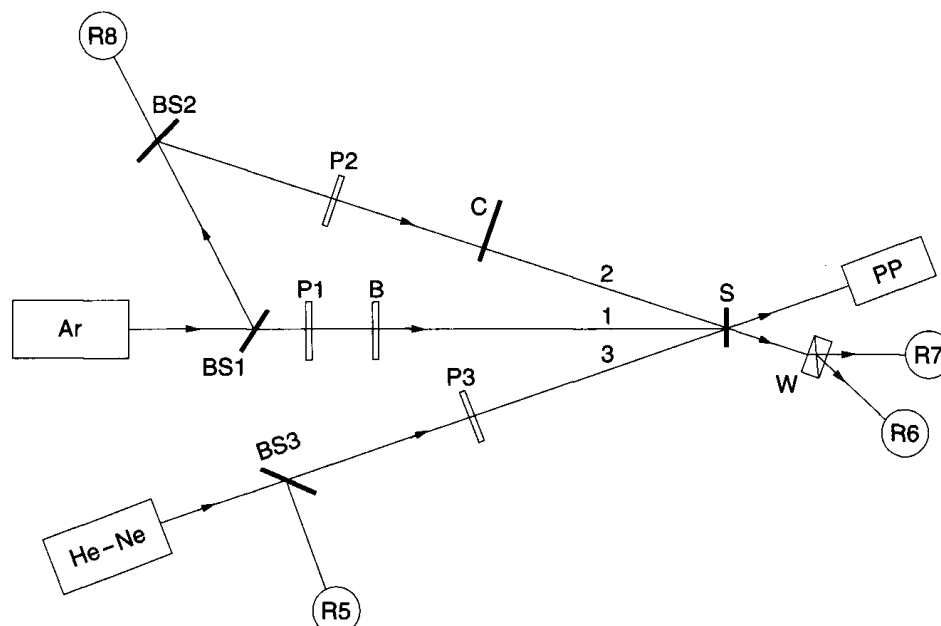


Figure 2 Experimental setup: Ar and He–Ne, lasers; PP, photopolarimeter; BS1, BS2, BS3, beamsplitters; R5, R6, R7, R8, photosensors; P1, P2, P3, polarizers; B, Babinet–Soleil compensator; C, shutter; S, sample; W, Wollaston prism.

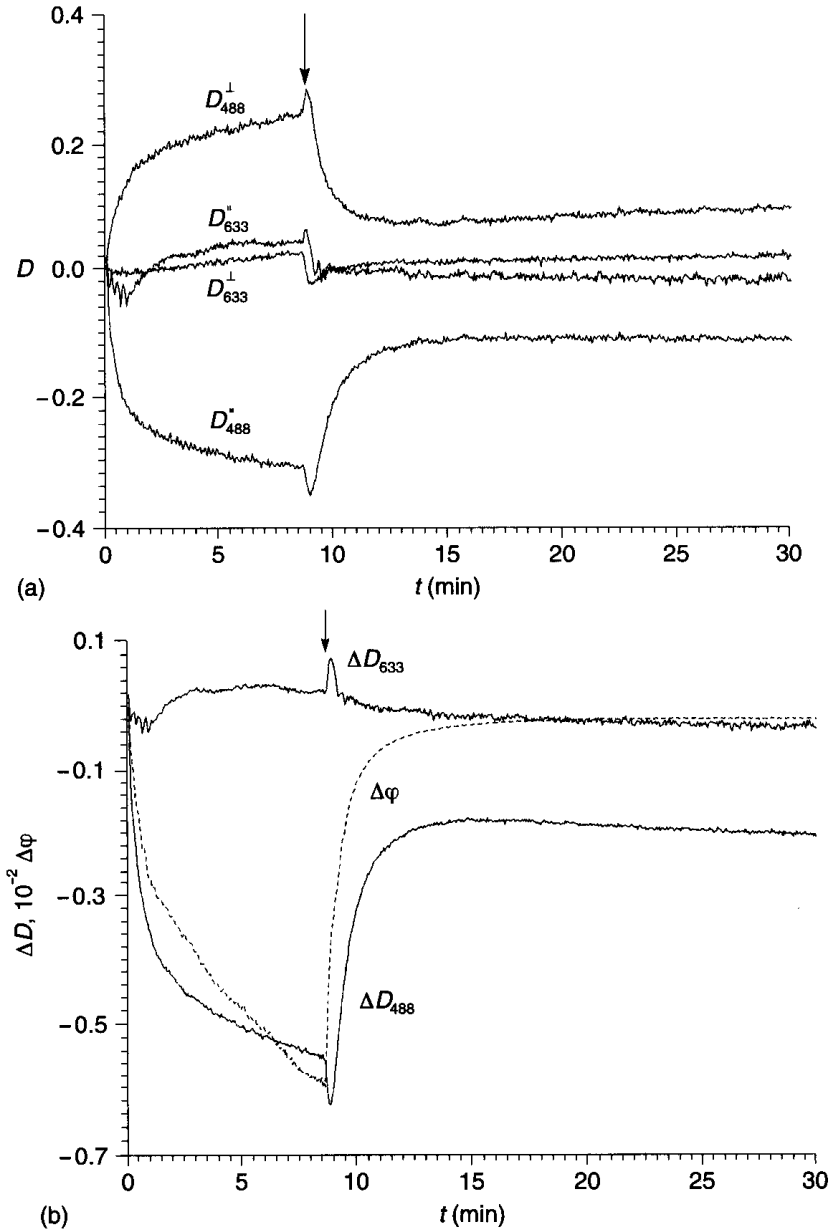


Figure 3 (a) The optical density for  $\lambda = 488$  nm and 633 nm on irradiation with an  $\text{Ar}^+$  laser at  $\lambda = 488$  nm, measured for light polarization parallel ( $\parallel$ ) and perpendicular ( $\perp$ ) to the irradiating beam polarization. (b) The photoinduced dichroism  $\Delta D$  for  $\lambda = 633$  nm and 488 nm and the anisotropic phase delay  $\Delta\varphi$  for 633 nm.

Part of the  $\text{Ar}^+$  beam is deflected by beam splitters BS1 and BS2 (beam 2) and its polarization is set to  $45^\circ$  by the polarizer P2. After passing through the sample this beam is split by a Wollaston prism W whose axes are vertical and horizontal. The two beams emerging from the prism fall on photosensors R6 and R7. Beam 3 from an He-Ne laser, linearly polarized at  $45^\circ$  by polarizer P3, also falls on the sample, and subsequently on a photopolarimeter PP that measures the Stokes parameters in real time [11, 12]. The signals from the photosensors

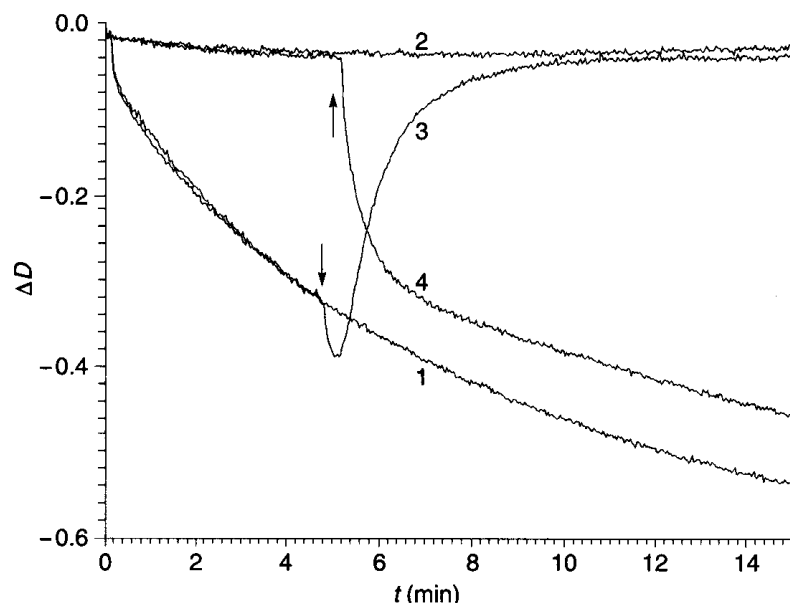


Figure 4 The photoinduced dichroism  $\Delta D$  on irradiation with linearly polarized light (curve 1); circularly polarized light (curve 2); linearly polarized light before the time indicated by an arrow and circularly polarized light after that time (curve 3); and circularly polarization first and then with light of linear polarization (curve 4).

and the photopolarimeter PP through an 8-channel analogue-to-digital converter (ADC) are fed to a personal computer (PC). From the data from R6 and R7, the photoinduced dichroism for  $\lambda = 488$  nm is calculated, and from the four Stokes parameters are calculated the photoinduced dichroism and birefringence for  $\lambda = 633$  nm, using the technique described in [13]. R5 and R8 are normalizing photosensors compensating for the instability in the intensity of the laser radiation. The photo-shutter C opens for 0.1 s, the interval between the individual measurements being 3 s. This minimizes the influence of the measuring  $\text{Ar}^+$  beam on the photoprocess. The influence of the measuring He-Ne beam is negligible because its wavelength is practically outside the absorption band of the dye. The intensities of the exiting beam and the two measuring beams are  $I_1 = 800 \text{ mW cm}^{-2}$ ,  $I_2 = 12 \text{ mW cm}^{-2}$  and  $I_3 = 60 \text{ mW cm}^{-2}$ , respectively.

The photoinduced changes in the optical parameters of the film are plotted in Figs 3a and 3b. Figure 3a illustrates the changes of the optical densities at  $\lambda = 488$  nm and 633 nm for light components polarized parallel ( $D^{\parallel}$ ) and perpendicular ( $D^{\perp}$ ) to the polarization direction of the exiting light. At the time designated by an arrow, the polarization of the exiting beam changes from linear to circular. The initial densities for the two wavelengths are  $D_0(488) = 0.76$  and  $D_0(633) = 0.07$ , respectively. The changes in the measured densities  $D^{\parallel}$  and  $D^{\perp}$  for  $\lambda = 488$  nm are substantial. They are similar but have opposite signs. At the same time, the changes in the average density at both wavelengths are negligible ( $\pm 0.03$ ).

Figure 3b displays the change in the dichroism  $\Delta D = D^{\parallel} - D^{\perp}$  and in the anisotropic phase delay, due to the birefringence,  $\Delta\varphi = 2\pi(n_{\parallel} - n_{\perp})d/\lambda$ , where  $n_{\parallel}$  and  $n_{\perp}$  are the refractive indices for light polarized along and perpendicular to the polarization direction of the acting light and  $d$  is the sample thickness. In a separate experiment the kinetics of the birefringence  $\Delta n$  for  $\lambda = 488$  nm were measured and practically coincide with the kinetics for  $\lambda = 633$  nm shown in Fig. 3b.

A series of experiments was carried out on the same type of samples in order to elucidate the influence of linearly or circularly polarized light. Figure 4 shows the kinetic curves of photo-

dichroism at  $\lambda = 488 \text{ nm}$  ( $600 \text{ mW cm}^{-2}$ ) on irradiation with linearly polarized exiting beam (curve 1), with a circularly polarized exiting beam (curve 2), and with linearly and circularly polarized light in succession (curve 3), and vice versa (first with circular and then with linearly polarized light) (curve 4). The results from these measurements correlate with the changes in the birefringence at  $\lambda = 633 \text{ nm}$  and with the photoinduced dichroism for both wavelengths. It can be seen that when the illumination with linearly polarized light is more prolonged and of higher intensity (Figs 3a and 3b) there is some memory effect in the photodichroism that is not observed in Fig. 4.

### 3. Discussion

The considerable value of the photoinduced dichroism ( $\Delta D$  reaches 0.6 at  $\lambda = 488 \text{ nm}$ ) is noteworthy, the changes in the average value of  $D$  remaining insignificant (within experimental error). Therefore, irradiation with linearly polarized light brings about reordering of the molecules. Since the absorption spectra of the dye molecules in the *trans* and *cis* forms are very close, these experiments alone are not sufficient to determine whether the ordered molecules are in *trans* or *cis* form. Most probably, they exist in both forms. The major result is that the curves of  $\Delta D(t)$  and  $\Delta\varphi(t)$  (Fig. 3b) during the photoprocess differ. Hence, the birefringence is not only caused by the photoinduced dichroism. It is known that during light irradiation, multiple isomerization of the molecules from *trans* into *cis* form and vice versa takes place. Probably some re-formation of the matrix also occurs in accordance with the optically induced ordering of the dye molecules. Evidence of such a process is the difference in curves 1 and 4 in Fig. 4. After the samples has been irradiated with circularly polarized light (which does not lead to dichroism), on irradiation with linearly polarized light, dichroism is induced much more quickly. This shows that the preliminary irradiation prepares the matrix so that it exercises smaller resistance to molecular rotation (or to the molecules' rotating parts). Especially interesting is the difference in the curves of  $\Delta\varphi(t)$  and  $\Delta D(t)$  on changing the exiting light polarization from linear to circular. Initially, the circularly polarized light strongly enhances the dichroism. It should be noted that such peculiarity is observed only at relatively high intensities ( $>400 \text{ mW cm}^{-2}$ ) of exiting light. It is known from polarization spectroscopy that photochemical equilibria depend on the polarization state of the exiting light [14]. For the *trans*–*cis* isomerization in the investigated dye/polymer layers we have observed that at high excitation levels with circularly polarized light leads to dependence of the photoreactions on the type of light at higher concentrations of the photoproduct. We think that this is the cause of the observed peculiarities in  $D^{\parallel}$ ,  $D^{\perp}$  and  $\Delta D$  (Figs 3a, 3b and 4). When the process is close to saturation after prolonged irradiation with linearly polarized light, the circularly polarized light excites new amounts of *trans* molecules that have been oriented in such a way that they were slightly affected by the linearly polarized light. On the other hand, by that moment the matrix is reordered in accordance with the irradiating linearly polarized light and the newly-excited molecules take on orientations enhancing dichroism. After irradiation with the circularly polarized light, this ordering disappears gradually and  $\Delta D$  and  $\Delta n$  gradually diminish.

Further detailed investigations of the influence of the exiting light intensity, dye concentration, matrix temperature and moisture will help better understand the stage of the photoprocess itself and the influence of the matrix.

### Acknowledgements

The authors are indebted to Dr Tz. Petrova for the useful discussions. This investigation is funded by Contracts F-61 and F-52 of the National Fund for Scientific Investigations.

## References

1. T. TODOROV, N. TOMOVA and L. NIKOLOVA, *Opt. Commun.* **47** (1983) 123; T. TODOROV, L. NIKOLOVA and N. TOMOVA, *Appl. Opt.* **23** (1984) 4309; T. TODOROV, L. NIKOLOVA, N. TOMOVA and V. DRAGOSTINOVA, *IEEE J. Quantum Electron.* **QE-22** (1986) 1262; N. TOMOVA, L. NIKOLOVA, V. DRAGOSTINOVA and T. TODOROV, *SPIE* **1183** (1989) 268.
2. I. D. SHATALIN, V. I. KAKICHASHVILI and Sh. D. KAKICHASHVILI, *Pisma ZTF* **13** (1987) 1051 (in Russian).
3. A. I. ZELTOV, B. I. STEPANOV and V. G. SHAVERDOVA, *Z. Prikl. Spektrosk.* **52** (1990) 280 (in Russian).
4. I. D. SHATALIN, *Opt. Spectrosc.* **66** (1989) 362.
5. T. LUCHEMEYER and H. FRANKE, *Appl. Phys. Lett.* **53** (1989) 2017.
6. Y. SHI, W. STEIER, L. YU, M. CHEN and L. DALTON, *Appl. Phys. Lett.* **59** (1991) 2935.
7. S. HVILSTED, F. ANDRUZZI and P. S. RAMANUJAM, *Opt. Lett.* **17** (1992) 1235.
8. P. S. RAMANUJAM, S. HVILSTED and F. ANDRUZZI, *Appl. Phys. Lett.* **62** (1992) 1041.
9. P. ROCHON, J. GOSSELIN, A. NATANSOHN and S. XIE, *Appl. Phys. Lett.* **66** (1992) 4.
10. E. MOHAJERANI, E. WHALE and G. R. MITCHELL, *Opt. Commun.* **92** (1992) 403.
11. T. TODOROV and L. NIKOLOVA, *Opt. Lett.* **17** (1992) 358.
12. L. NIKOLOVA, M. IVANOV, T. TODOROV and S. STOYANOV, *Bulg. J. Phys.* **20** (1993) 304.
13. L. NIKOLOVA, T. TODOROV, P. SHARLANDJIEV and S. STOYANOV, *Appl. Opt.* **31** (1992) 6698.
14. V. A. GAISENOK and A. M. SARJEVSKI, *Anisotropy of the absorption and luminescence of polyatomic molecules*, Minsk, Universitetskoe, 1986 (in Russian).